

# Leveraging Transfer Learning Across Industrial and Medical Anomaly Domains: From Aircraft Fuselage Defect Detection to Chest X-ray Abnormality Identification

**Kien Vu Ngoc**

Academy of Military Science and Technology.

[kvu3009@gmail.com](mailto:kvu3009@gmail.com)

**Huy Dang Gia**

HUS High School for Gifted Students

doi: <https://doi.org/10.37745/ejcsit.2013/vol14n18596>

Published February 20, 2026

---

**Citation:** Ngoc K.V. and Gia H.D. (2026) Leveraging Transfer Learning Across Industrial and Medical Anomaly Domains: From Aircraft Fuselage Defect Detection to Chest X-ray Abnormality Identification, *European Journal of Computer Science and Information Technology*, 14(1), 85-96

---

**Abstract:** *Transfer learning (TL) enables knowledge learned in one domain to improve performance in another related domain; however, its application to industrial and medical anomaly detection (AD) is often limited by domain discrepancies and scarce labeled data. This research addresses these challenges by bridging Aircraft Fuselage Defect Detection (AFDD) and Chest X-ray (CXR) Abnormality Identification through cross-domain TL, enabling effective feature generalization between industrial and medical imaging tasks. Publicly available aircraft inspection images and CXR datasets are used to ensure diversity and representative anomalies. Data pre-processing incorporates adaptive histogram equalization (AHE) for contrast enhancement and median filtering (MF) to reduce noise, followed by image normalization to standardize input dimensions. For robust feature representation, Gray-Level Co-occurrence Matrix (GLCM) and Histogram of Oriented Gradients (HOG) are employed to capture complementary structural and texture information. The proposed Dynamic Grey Wolf Optimizer-driven Deep Convolutional Transform Network (DGWO-DCTN) integrates preprocessing, feature extraction, and AD into a unified framework. A DC Neural Network (DCNN) extracts hierarchical spatial features, while a Transformer module models long-range dependencies and global contextual relationships. To improve convergence and generalization, the DGWO adaptively tunes network hyperparameters and weights. TL is realized by fine-tuning the model on CXR data using pretrained knowledge from fuselage defect detection. Experimental evaluation implemented in Python demonstrates strong performance, achieving 94% precision, 93.75% recall, 96.80% accuracy, and a 93.80% F1-score. These results confirm that combining TL with hybrid deep architectures provides an effective and computationally efficient solution for cross-domain AD.*

**Keywords:** cross-domain, industrial inspection, medical imaging, abnormality identification, computer vision.

---

## INTRODUCTION

The AFDD and CXR abnormality identification are two important AD tasks in industrial inspection and medical diagnosis. When it comes to aircraft maintenance, the maintenance team should identify defects, including cracks, corrosion, and dents in the fuselage to maintain the structural safety of the aircraft and avoid disastrous failures [1]. Automated image based inspection systems are rapidly being implemented to enhance the level of accuracy in detection and also lessening the use of manual inspection particularly on the subtle and rare defects. Likewise, CXR imaging is a diagnostic instrument that has been used extensively in the diagnosis of the thoracic abnormalities including pneumonia, lung nodules, and effusion [2, 3].

Nevertheless, CXRs have low contrast with a high overlap and limited anatomically expertly annotated data which makes them difficult to interpret properly. Such factors usually have an impact on the reliability and consistency of diagnosis. Although aircraft fuselage image and CXRs are in the different fields, the images have common features such as localized abnormalities barely noticeable, complicated backgrounds, and extreme imbalance of classes. TL can be used to leverage these similarities, to apply knowledge acquired by AFDD to CXR abnormality detection. This inter-domain strategy assists in enhancing performance of detection and generalization in medical imaging and also lowering the requirements of the large labeled datasets [4, 5].

This research investigates cross-domain TL by transferring knowledge from AFDD to CXR abnormality identification. By utilizing shared low- and mid-level visual features, the approach improves learning efficiency and detection accuracy, demonstrating the potential of unified anomaly detection (UniAD) across industrial and medical domains. The objective of the proposed research is to build the proposed DGWO-DCTN framework to deliver a robust and accurate AD across heterogeneous domains. The research aimed at applying TL as a means of successfully generalizing the knowledge acquired in the field of AFDD to identify the abnormalities in the CXRs.

## LITERATURE REVIEW

A comparative overview of recent industrial and medical abnormality detection and classification methods is presented in table 1 and includes goals, data sets, methodology, pivotal findings and constraints of the current methodologies and strategies.

**Table 1: Summary of Related studies**

Ref. no	Objective	Data	Method	Result	Limitation
[6]	Localize CXR abnormalities	NIH CXR (112k), VinDr-CXR (18k)	Self-supervised BarlowTwins-CXR (SS)	+3% mAP@50 vs ImageNet-based TL	Limited datasets, single backbone
[7]	Detect symmetric CXR abnormalities	Public CXR dataset (14 classes)	Dual Attention (DA) + multi-scale feature fusion	Average precision (AP) = 0.362	Single dataset validation
[8]	Cross-domain AD	Medical (MRI, CT, OCT), Industrial (MVTec AD)	Unsupervised Multi-component Unsupervised AD (Multi-AD) Convolutional Neural Network with Squeeze-and-Excitation attention, knowledge distillation, and T-S architecture	High localization accuracy at image and pixel levels across domains	Higher training complexity due to multi-network design
[9]	Unified multi-class AD	MVTec-AD, CIFAR-10	UniAD with feature jittering, masked attention, and layer-wise query decoder	Improved detection and localization (96.5% / 96.8% on MVTec-AD)	Performance may degrade under large domain shifts

The research addresses the above gaps that exist in the field by providing the ability to perform cross-domain TL of both industrial and medical images, as well as a better generalization with limited labeled data. The DCNN-Transformer with DGWO hybrid is robust in terms of feature learning, convergent stability and efficient at detecting anomalies.

## METHODOLOGY

The DGWO-DCTN framework combines preprocessing, feature extraction, and deep learning (DL) into a unified cross-domain AD pipeline. DCNN and Transformer networks learn local and global features, DGWO optimizes model parameters, and TL enables knowledge transfer from AFDD to CXR abnormality detection. Figure 1 shows the end-to-end workflow from data collection and preprocessing to feature extraction, DL, and AD results.

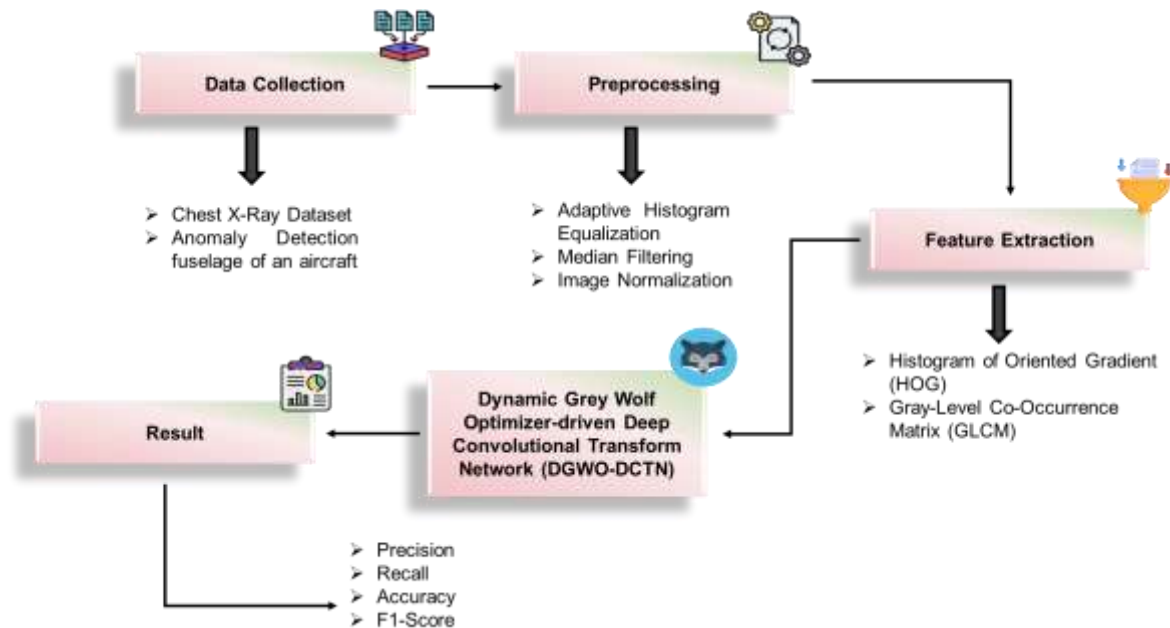


**Figure 1: Overall Workflow of the DGWO-DCTN**

### Dataset

The data set's CXR images are categorized into four groups: normal, pneumonia, COVID-19, and tuberculosis. The CXR images of patients who have been diagnosed with either the normal class or the corresponding condition match the classes. The dataset is intended to be helpful in medical image analysis research, particularly in the automated identification and categorization of respiratory conditions. Source: (<https://www.kaggle.com/datasets/pritpal2873/chest-x-ray-dataset-4-categories>).

The data is fundamentally applied in detecting anomalies in the fuselage of an aircraft manufacturer company. Recorded the data on the mockup of the fuselage by multiple experimentations at varying distances of the mockup. The dataset simply consists of the scans of mockups that have been scanned top to bottom and with or without anomalies.

Figure 2 represents a representative (a) CXR and (b) AFDD image used for abnormality detection in the proposed framework. Also the collected both data splitted into training 75% and validation 25%.

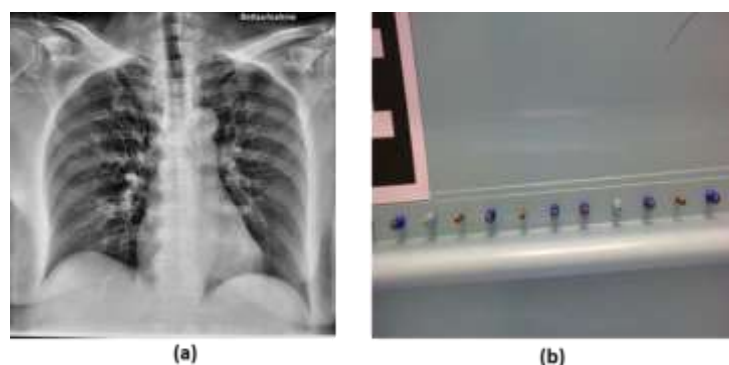


**Figure 2: Sample of (a) CXR and (b) AFDD**

### Data Pre-processing

The preprocessing pipeline that improves image quality and minimizes domain discrepancies between CXR and airplane fuselage images. To promote feature consistency and facilitate efficient cross-domain translation, contrast enhancement, noise reduction, and intensity normalization are used.

**AHE:** AHE is applied to both aircraft fuselage defect images and CXR scans to normalize local intensity variations and enhance fine structural details across domains. The enhancement process is regulated using global image entropy,

$$F = -\sum_l^{255} p_l \log_2(p_l) \quad (1)$$

In Equation (1),  $p_l$  denotes the probability of gray level  $l$ , and  $F$  stands for image entropy. Entropy-guided adjustment ensures optimal contrast amplification, suppresses noise over-enhancement, reduces domain-induced visual discrepancies, and enables effective transfer of defect-relevant features from fuselage inspection to CXR abnormality identification.

**MF:** MF is employed as a nonlinear spatial denoising technique to remove impulsive and random noise while preserving edge and structural information in aircraft fuselage defect images and CXR scans. The filtered pixel value at location  $e'(s, k)$  is computed as

$$e'(s, k) = \underset{(q,r) \in Q_{sk}}{\text{median}} \{h(q, r)\} \quad (2)$$

Where  $h(q, r)$  denotes the intensity values within the neighbourhood  $\underset{(q,r) \in Q_{sk}}{\text{median}}$  in Equation (2). By changing the median for every pixel of its surrounding intensities, the filter effectively suppresses noise without causing excessive smoothing of defect boundaries or anatomical structures, thereby enhancing image reliability, reducing inter-domain variability, and improving feature stability for cross-domain TL and AD.

**Image normalization using Z-score normalization:** To standardize pixel intensity distributions and reduce variances brought on by various imaging conditions, sensors, and acquisition settings, Z-score normalization is applied to CXR scans and aircraft fuselage defect images. Each pixel intensity is normalized as

$$P_{new} = \frac{P - \mu}{\sigma} = \frac{P - \text{Mean}(P)}{\text{StdDev}(P)} \quad (3)$$

In Equation (3),  $\mu$  is the mean intensity,  $P$  is the original pixel value, and  $\sigma$  is the standard deviation,  $P_{new}$  Normalized pixel value after Z-score normalization. The Figure 3 (a) CXR and (b) AFDD image is shows both before and after preprocessing.

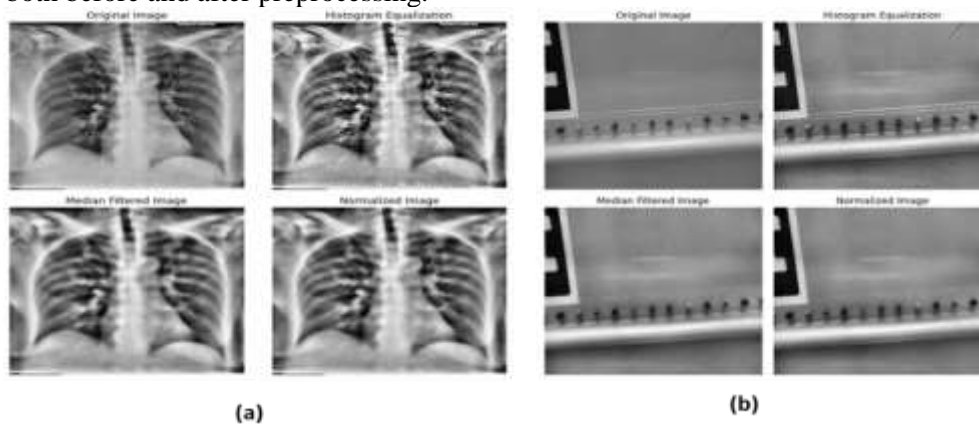


**Figure 3: Pre-processing Stages of (a) CXR and (b) AFDD**

**Feature Extraction**

The both HOG and GLCM features are obtained to obtain the complementary structural and texture information of aircraft fuselage defects in images and CXR scans. These crafted features increase feature strength, decrease domain changeability, enable successful cross-domain transfer study and anomaly recognition.

**HOG:** HOG features are used to capture local texture and structural information in aircraft fuselage defect images and CXR scans by analyzing edge orientation and gradient distribution. Image gradients are computed using Sobel operators, and the gradient magnitude and orientation are given by

$$b(u, d) = \sqrt{c_u^2(u, d) + c_d^2(u, d)}, \theta(u, d) = \tanh^{-1} \left( \frac{c_d(u, d)}{c_u(u, d)} \right) \tag{4}$$

$c_d(u, d)$  and  $c_u(u, d)$  represent horizontal and vertical gradients.  $b(u, d)$  Gradient magnitude at pixel location  $(u, d)$ , representing the strength of local intensity change,  $\theta(u, d)$  Gradient orientation at pixel location  $(u, d)$ , indicating the direction of the edge.  $\tanh^{-1}(\cdot)$  Inverse tangent function used to compute gradient direction shown in Equation (4). HOG descriptors capture local edges and textures, improving defect/pathology discrimination and supporting cross-domain transfer learning.

**GLCM:** GLCM is a second order statistical texture feature extraction method of modeling the spatial relations between pairs of pixel intensities at predetermined distances and orientations. For an image quantized to  $M_h$  gray levels, the GLCM  $H(j, i | \Delta y, \Delta x)$  represents the frequency of occurrence of a pixel with intensity  $i$  having a neighboring pixel with intensity  $j$  separated by an offset  $(\Delta y, \Delta x)$ . Directional GLCMs are calculated at a variety of orientations (*e.g.*,  $0^\circ, 45^\circ, 90^\circ, 135^\circ$ ) to detect anisotropic texture patterns and structure variability). GLCM-based statistical descriptors (contrast, correlation, energy, homogeneity) capture subtle texture and structural variations, enhancing feature robustness, reducing domain variability, and improving cross-domain AD for defects in images like aircraft fuselage and CXR scans. Figure 4 illustrates how pixel intensity pairs are mapped to form a GLCM for texture representation. Figure 5 shows texture and structural patterns in a (a) CXR and (b) AFDD image.

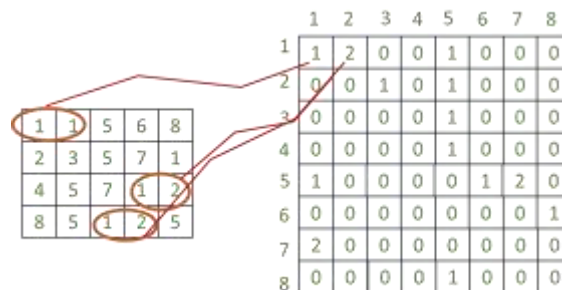


**Figure 4: Construction of GLCM**

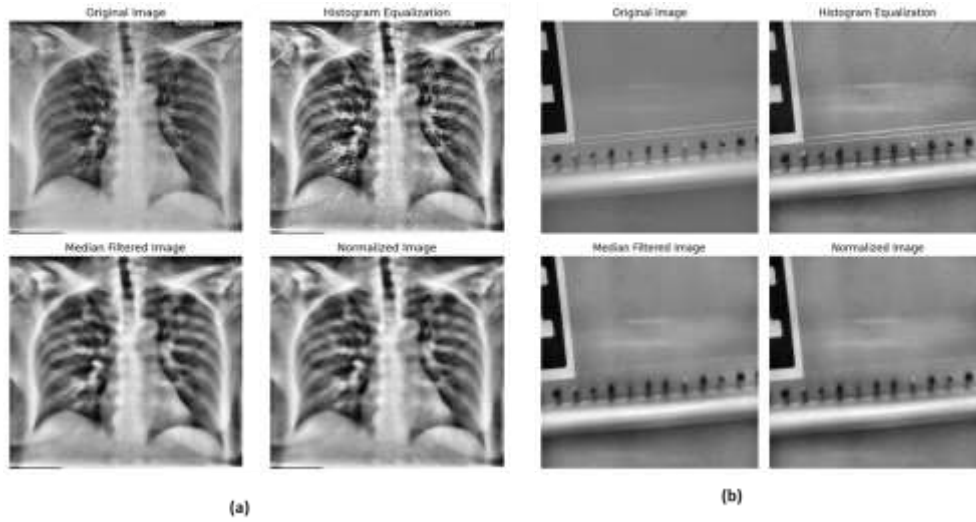


**Figure 5: Texture and Structure of (a) CXR Image and (b) AFDD**

#### **DGWO-DCTN Architecture for Cross-Domain AD**

The DGWO-DCTN framework is introduced, which incorporates a DCNN to learn local features, TN to learn global contextual dependencies, and DGWO to optimize the parameters. The integrated architecture permits the effective extraction of both local and global representations, as well as guarantees effective convergence and robust cross-domain TL towards AD.

**DCNN:** The DCNN is used to identify hierarchical spatial characteristics of aircraft fuselage defects images and CXR images. This network can learn low-level textural features, middle-level structural patterns, and high-level semantic representations since it is made up of multiple convolutional layers, max-pooling layers in between, and finally fully connected layers. The activation functions used are Rectified Linear Unit that make the process nonlinear and increase generalization and convergence as well as dropout regularization to reduce overfitting. The DCNN is first trained on aircraft fuselage defect data to learn the feature representations of defect relevance, and then fine-tuned on the CXR samples. It is a weight refinement process that allows the effective cross-domain TL process through reuse of shared structural properties and adaptation of domain specific features, enhancing the performance of the AD in heterogeneous industrial and medical imaging domains.

**TN:** The TN is combined in order to formulate the global contextual information and long-range spatial dependencies of aircraft fuselage defect images and CXR scans. In contrast to convolutional layers where interactions between localized receptive fields and the localization of details are considered, the self-attention mechanism of the TN includes the ability to capture interactions between spatially distant regions and allows the effective representation of distributed, subtle, and context-dependent anomalies. Such global dependency modelling can be especially useful in locating elongated fuselage defects and diffuse pathological patterns in the CXR images that cannot be identified well using local feature extraction. The transformation of the feature in the TN is as follows:

$$Z_{output} = LayerNorm(Z \oplus Q_{TM}) \quad (5)$$

In Equation (5),  $Z$  represents the learned feature matrix,  $Q_{TM}$  denotes positional encoding,  $\oplus$  indicates element-wise addition, and  $LayerNorm(\cdot)$  stabilizes training and enhances global contextual feature representation for AD. Layer normalization makes training more stable, and convergence faster, and

global contextual representations more robust, which is useful in cross-domain TL and accurate AD in both industrial and medical imaging applications.

**DGWO:** DGWO is used to optimize deep model parameters trained on aircraft fuselage defect images and CXR scans, eliminating early convergence and lack of exploration in standard DGWO. DGWO enhances search diversity and convergence, by integrating global leadership with neighborhood-based learning, to facilitate effective cross-domain TL between AFDD and CXR abnormality detection. The status of every search agent is changed to:

$$Y^{a+1} = \text{agr} \min\{e(Y_{GWO}^{a+1}), e(Y_{DLH}^{a+1})\} \quad (6)$$

$Y_{GWO}^{a+1}$  denotes the candidate position obtained from the standard *GWO* mechanism,  $Y_{DLH}^{a+1}$  represents the position learned from neighboring agents, and  $e(\cdot)$  is the fitness function presented in Equation (6). In the framework proposed, DGWO is able to optimize deep network parameters and hyperparameters, which enables to maintain a stable convergence and strong generalization to achieve the successful cross-domain TL of image-based AFDD and X-ray abnormality image detection in the chests.

The incorporated DGWO-DCTN used to learn local features, model the global context with Transformer, and optimize the parameters. This architecture allows cross-domain TL to perform and AD to be correct in the aircraft fuselage, CXR images.

### Transfer Learning Strategy

DGWO-DCTN framework is initially pretrained on the AFDD dataset and trained to identify fuselage defects and extract sound structural characteristics. This prior knowledge is then trained on the CXR dataset and the model is able to adapt to the medical anomalies whilst utilizing the prior learned representations, enhancing generalization and shortening the convergence between domains.

## RESULT

Using Python-based implementation, the results demonstrate accurate and consistent AD for both CXR abnormality identification and AFDD. Performance metrics, confusion matrices, PR/ROC curves, and convergence plots confirm stable learning and effective cross-domain knowledge transfer. The comparative analysis also highlights improved accuracy with reduced testing time, indicating computational efficiency.

**Confusion Matrix:** Figure 6 shows the confusion matrices for both (a) CXR abnormality identification and (b) AFDD exhibit strong diagonal dominance, indicating accurate classification with minimal errors. This reflects effective feature learning in the industrial domain and successful knowledge transfer to the medical domain for reliable cross-domain AD.

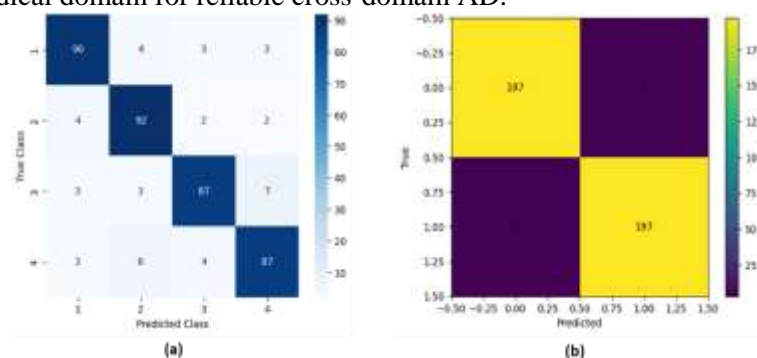
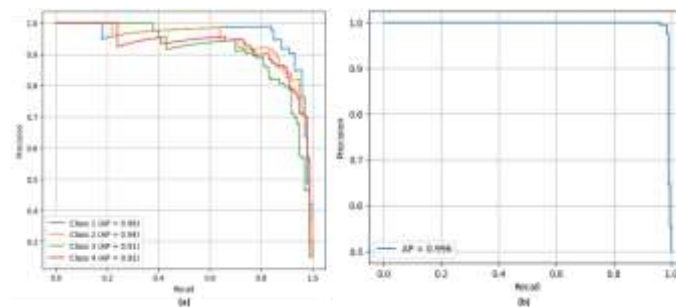


Figure 6: Confusion Matrix of DGWO-DCTN

**Precision–Recall (PR):** Figure 7 illustrates the PR curves for (a) CXR abnormality identification and (d) AFDD, demonstrating high average precision across all classes. The curves show strong precision retention at higher recall levels, confirming reliable anomaly discrimination and consistent performance across both medical and industrial domains, supporting effective cross-domain AD.



**Figure 7: PR Curves for (a) CXR and (b) AFDD**

**Receiver Operating Characteristic (ROC) Analysis:** Figure 8 presents the ROC curves for (a) CXR abnormality identification and (b) AFDD. Strong discriminative capacity and dependable AD performance across both medical and industrial domains are demonstrated by the curves' high true positive rates and low false positive rates, which lead to high AUC values.

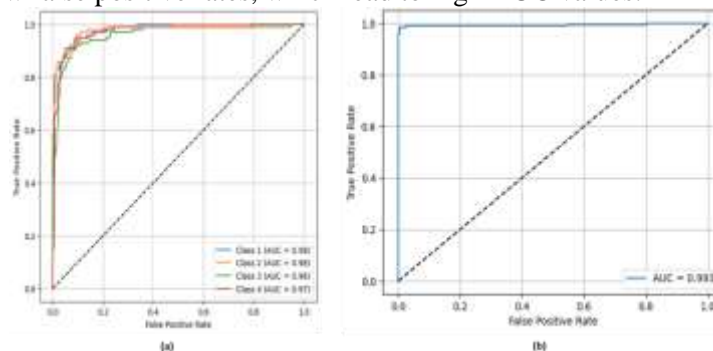


**Figure 8: ROC Curves for (a) CXR and (b) AFDD**

**Training Vs Validation Accuracy and Loss:** The accuracy and loss curves for training and validation are shown in Figure 9 for both (a) AFDD and (b) CXR abnormality diagnosis. The results show stable convergence with minimal performance gap between training and validation, indicating effective learning, reduced overfitting, and strong generalization across medical and industrial domains.

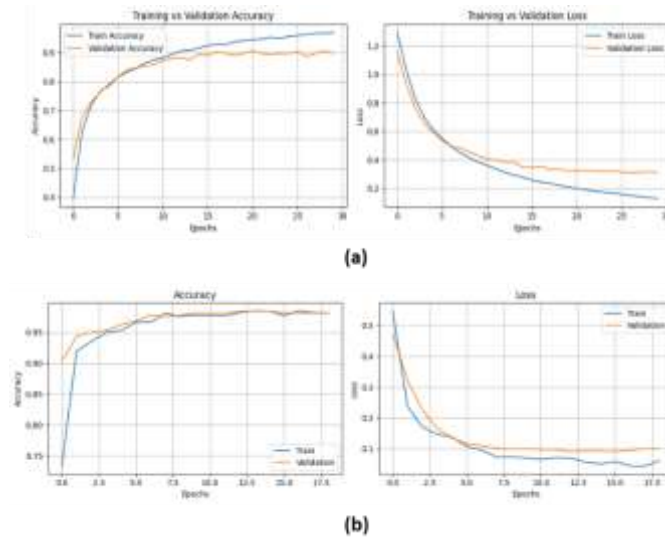


**Figure 9: Model Convergence Analysis for (a) CXR and (b) AFDD**

**Comparative Analysis**

**Precision:** The percentage of correct cases of abnormality detected out of the total predicted abnormal cases, which depicts the trustworthiness of positive predictions in both data.

**Recall:** The capability of the model to identify real abnormal cases in a correct manner, which is indicative of sensitivity to anomalies.

**Accuracy:** By calculating the number of correctly classified samples relative to the total data of both samples, it indicates the overall accuracy of the model.

**F1-Score:** It gives a balanced measure of accuracy and recall particularly where there are imbalanced class distributions. Table 2 and Figure 10 (a) shows that DGWO-DCTN achieves better in metrics compared to baseline models.

**Table 2: Cross-Domain Overall Model Performance**

Model	Precision (%)	Recall (%)	Accuracy (%)	F1-score (%)
DCNN	91.0	90.2	91.5	90.6
DCNN + Transformer	92.5	92.0	93.0	92.2
<b>DGWO-DCTN [Proposed]</b>	<b>94.0</b>	<b>93.75</b>	<b>96.8</b>	<b>93.8</b>

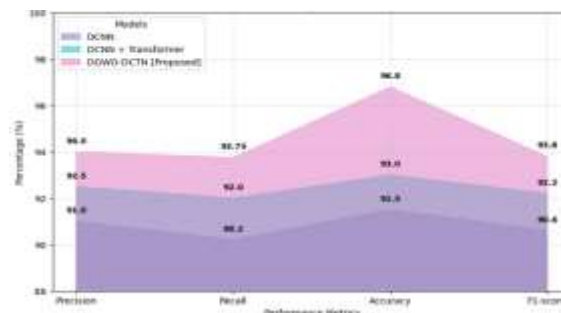


**Figure 10: Model Performance Evaluation**

The results show that DGWO-DCTN achieves the higher in metrics, demonstrating its effectiveness. This confirms that cross-domain transfer learning from AFDD to CXR enhances feature representation and improves AD performance.

## DISCUSSION

Multi-AD achieves strong detection performance; however, the architecture with knowledge distillation increases computational and training complexity and remains sensitive to severe domain shifts or highly diverse anomaly distributions [8]. Whereas the unified model applies well to UniAD and offers high performance, the attention-based and various improvement modules augment the complexity of computations and training costs. Moreover, it is only tested on industrial style datasets and its extrapolation to medical or highly heterogeneous areas is unclear [9]. The research is able to circumvent the discrepancy of domains and scarce labeled data due to the cross-domain transfer learning that is utilized to share the features of anomalies between aircraft fuselage images and chest X-ray images. The hybrid DCNN-Transformer model, which is optimized by DGWO, contributes to better generalization, convergence, and computational efficiency to conduct reliable cross-domain AD.

## CONCLUSION

Research aims to design a powerful framework of cross-domain anomaly detectors by employing a TL method for AFDD to detect abnormalities in the CXRs with the proposed DGWO-DCTN model. Images of aircraft inspections publicly available and the CXR data of pneumonia, tuberculosis, COVID-19, and normal cases were utilized. AHE methods, median filtering, and Z-score normalization was performed, and features of HOGs and GLCMs were extracted. In terms of accuracy and efficiency, the suggested DGWO-DCTN framework outperformed the existing approaches with 94% accuracy, 93.75% recall, 96.80% accuracy, and 93.80% F1-score. Research used limited public datasets and only 2D X-ray images without multimodal data or explainability. Future work can use larger datasets, integrate explainable AI and multimodal clinical data, and enhance real-time clinical applicability.

## REFERENCE

1. Brandoli, B., de Geus, A.R., Souza, J.R., Spadon, G., Soares, A., Rodrigues Jr, J.F., Komorowski, J. and Matwin, S., 2021. Aircraft fuselage corrosion detection using artificial intelligence. *Sensors*, 21(12), p.4026. <https://doi.org/10.3390/s21124026>
2. Bhandary, A., Prabhu, G.A., Rajinikanth, V., Thanaraj, K.P., Satapathy, S.C., Robbins, D.E., Shasky, C., Zhang, Y.D., Tavares, J.M.R. and Raja, N.S.M., 2020. Deep-learning framework to detect lung abnormality—A study with chest X-Ray and lung CT scan images. *Pattern Recognition Letters*, 129, pp.271-278. <https://doi.org/10.1016/j.patrec.2019.11.013>
3. Zhang, J., Xie, Y., Pang, G., Liao, Z., Verjans, J., Li, W., Sun, Z., He, J., Li, Y., Shen, C. and Xia, Y., 2020. Viral pneumonia screening on chest X-rays using confidence-aware anomaly detection. *IEEE transactions on medical imaging*, 40(3), pp.879-890. <https://doi.org/10.1109/TMI.2020.3040950>
4. Upadhyay, A., Li, J., King, S. and Addepalli, S., 2023. A deep-learning-based approach for aircraft engine defect detection. *Machines*, 11(2), p.192. <https://doi.org/10.3390/machines11020192>
5. Ho, T.K.K. and Gwak, J., 2020. Utilizing knowledge distillation in deep learning for classification of chest X-ray abnormalities. *IEEE access*, 8, pp.160749-160761. <https://doi.org/10.1109/ACCESS.2020.3020802>
6. Sheng, H., Ma, L., Samson, J.F. and Liu, D., 2024. BarlowTwins-CXR: enhancing chest X-ray abnormality localization in heterogeneous data with cross-domain self-supervised learning. *BMC Medical Informatics and Decision Making*, 24(1), p.126. <https://doi.org/10.1186/s12911-024-02529-9>

7. Liu, D., Lu, S., Zhang, L. and Liu, Y., 2023. Anomaly detection in chest X-rays based on dual-attention mechanism and multi-scale feature fusion. *Symmetry*, 15(3), p.668.<https://doi.org/10.3390/sym15030668>
8. Rahmانيar, W. and Suzuki, K., 2025. Multi-AD: cross-domain unsupervised anomaly detection for medical and industrial applications. *Pattern Recognition*, 172, p.112486.<https://doi.org/10.1016/j.patcog.2025.112486>
9. You, Z., Cui, L., Shen, Y., Yang, K., Lu, X., Zheng, Y. and Le, X., 2022. A unified model for multi-class anomaly detection. *Advances in Neural Information Processing Systems*, 35, pp.4571-4584.<https://doi.org/10.48550/arXiv.2206.03687>